Characterization of Nonvolatile Switches Based on 2-D Multilayered hBN Memristors for High-Frequency Applications

Jordi Verdú[®], Senior Member, IEEE, Tobías Amarilla[®], Yaqing Shen, Graduate Student Member, IEEE, Sebastian Pazos, Member, IEEE, Mario Lanza[®], Fellow, IEEE, and Pedro de Paco[®], Senior Member, IEEE

Abstract-RF/microwave systems with large number of elements usually require switching elements with very small footprint, but providing very good electrical performance, low switching times, and good power-handling capabilities. In this sense, nonvolatile switches based on 2-D materials are emerging as a very suitable alternative to CMOS or MEMS-based technologies, mainly due to the capability of keeping a certain state with no energy consumption. In this article, different switches have been designed and fabricated using a multilayered structure based on 18 2-D hexagonal boron nitride (hBN) layers on three different substrates, high-resistivity silicon, quartz, and polycrystaline CVD diamond. The proposed device has been characterized in a frequency range up to 26.5 GHz for these three substrates. The ON-state resistance and OFF-state capacitance have been extracted from experimental data using an equivalent electric model being 28 Ω and 22 fF, leading to insertion losses (ILs) better than 2.5 dB in case of CVD diamond, and isolation better than 10 dB in case of quartz, for the ON- and OFF-states, respectively.

Index Terms—2-D materials, hexagonal boron nitride (hBN) resistive switch, nonvolatile switch.

I. INTRODUCTION

THE use of RF/microwave switches is very intensive as a basic building block in a very wide range of systems, from end-user terminals to satellite payloads, for applications related to the RF signal routing or sophisticated redundancy schemes to improve reliability [1], [2], [3], [4]. The most popular technologies available to implement the switch are based on semiconductor or mechanical approaches. CMOS siliconon-insulator (SOI) [5], [6] provides miniaturized footprints and low-cost integration; however, they exhibit limitations related to power-handling, linearity, or high insertion losses (ILs). Some of these limitations can be overcome using

Received 10 January 2025; accepted 25 January 2025. Date of publication 17 June 2025; date of current version 17 September 2025. This work was supported by the Spanish Secretaría de Estado de Investigación, Desarrollo e Innovación under Grant PID2021-127203OB-I00. (Corresponding author: Jordi Verdú.)

Jordi Verdú, Tobías Amarilla, and Pedro de Paco are with the Department of Telecommunications and Systems Engineering-WavesLab, Universitat Autònoma de Barcelona, 08193 Cerdanyola del Vallès, Spain (e-mail: Jordi.Verdu@uab.cat).

Yaqing Shen and Sebastian Pazos are with the Physical Science and Engineering Division, King Abdullah University of Science and Technology (KAUST), Thuwal 23955, Saudi Arabia.

Mario Lanza is with the Department of Materials Science and Engineering, National University of Singapore, Singapore 117575 (e-mail: mlanza@nus.edu.sg).

Digital Object Identifier 10.1109/LMWT.2025.3576996

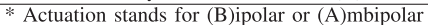
gallium nitride field-effect transistor (GaN-FET), thanks to the high breakdown voltage, large currents' handling, and wide dynamic range, providing the capability of blocking high voltages while maintaining good ILs and isolation at microwave frequencies, but a limited frequency range of operation at millimeter-wave applications [7], [8]. Moreover, microelectromechanical system (MEMS)-based switches [9], [10] present a very good RF performance; however, they require high operational voltages, longer switching time, and have some packaging limitations due to their bulky size. Phasechange materials (PCMs) have been consolidated during the past years in the design of switches for RF applications [11], [12]. These type of switches are controlled by means of a heater with independent terminals [13] which is the mechanism to bring the material from crystalline to amorphous state, thus switching the device between low- and high-resistance state, and vice versa. These devices have been demonstrated beyond 50 GHz [14], [15], with a reported endurance up to 10⁷ cycles in a single device; however, their integration in a large circuit must be done carefully due to thermal issues and may limit the performance above 24 GHz due to some parasitic capacitances [16].

As an alternative, 2-D materials are gaining attraction due to the low power consumption and reduced footprint in comparison to more standard solid-state devices [2]. Particularly, nonvolatile switches based on hexagonal boron nitride (hBN) [21], [22], [23] or molybdenum disulfide (MoS₂) [24] are of special interest due to the property of maintaining a certain state (ON/OFF) without requiring any constant voltage control signal which drastically reduces the energy consumption, which can be critical in RF systems with a large number of elements. A state-of-the-art comparison is given in Table I for the main nonvolatile technologies. While the performance in terms of frequency range, ILs) and isolation, R_{ON} resistance, or switching time are comparable or better than other technologies, the multilayer hBN technology is activated by means of ambipolar voltage. Unlike bipolar activation, no complex biasing network to switch both the polarities is needed which simplifies the required periphery for the bias network.

The objective in this work is focused on the performance of the device in the RF/microwave frequency domain. Different switches in series configuration as shown in Fig. 1 have been fabricated and experimentally characterized in a frequency range up to 26.5 GHz on different substrates: high-resistive

Ref.	Technology	Max. Voltage (Actuation*)	R _{ON} (Min)	Switching time (ns)	Frequency	IL (dB)	Isolation (dB)
[17]	Cu/Nafion	3 V (B)	9.2 Ω	N/A	10 GHz	0.6@10 GHz	20@10 GHz
[18]	Monolayer MoS2	1.5 V (B)	8 Ω	< 0.5	480 GHz	0.7@120 GHz	25@120GHz
[19]	Monolayer hBN	1.5 V (B)	1.4 Ω	< 0.5	210 GHz	0.5@180 GHz	10@210 GHz
[20]	Monolayer hBN	0.5 V (B)	5 Ω	10	170 GHz	0.5@170 GHz	22.5@170 GHz
T.W.	Multilayer hBN	<3 V (A)	5 Ω	< 2.5	260 GHz	0.9@120 GHz	10@120 GHz

TABLE I STATE OF THE ART FOR LOW-VOLTAGE SWITCHING TECHNOLOGIES AT HIGH FREQUENCIES



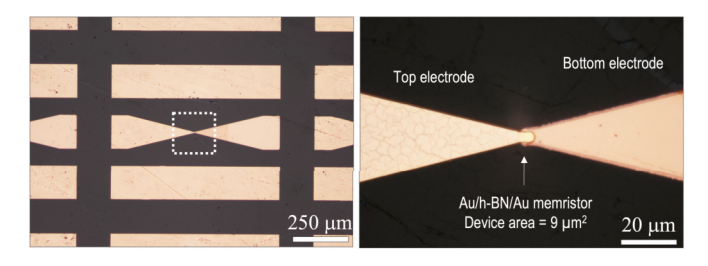


Fig. 1. Overview of the fabricated switch based on multilayer 2-D hBN (left). Zoom on the active area with size $9 \mu m^2$ [23].

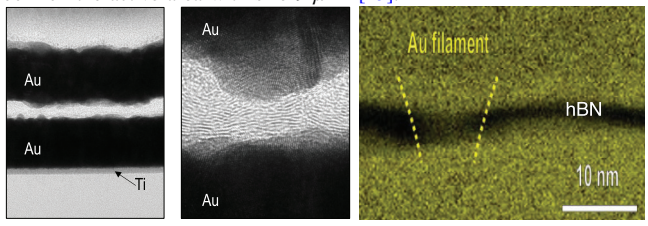


Fig. 2. (Left) SEM image of the multilayer hBN between metal electrodes. (Center) Detail of the hBN structure comprising 18 layers of 6-nm thickness each. (Right) Detail of the conductive nanofilament due to electron migration from metal into the insulator.

silicon, quartz, and polycrystaline chemical vapor deposition (CVD) diamond. First, the structure of the device, the principle of operation and set voltage conditions, and the electrical model are discussed. Next, the fabricated switches are characterized in the RF/microwave frequency domain up to 26.5 GHz for the ON- and OFF-states so the main parameters of the model are extracted. Finally, the conclusions are presented.

II. RF SWITCHES BASED ON MULTILAYER hBN: PRINCIPLE OF OPERATION AND DC CHARACTERIZATION

The proposed switch has been designed in a vertical metal-insulator–metal (MIM) configuration using an adhesion layer of titanium with a thickness of 5 μ m and gold for metal electrodes with a thickness of 50 μ m as shown in Fig. 2. The hBN resistive material comprises 18 layers with a total thickness of 6 nm and the active area is 3 × 3 μ m, and it has been fabricated on three different substrates: n-type 500- μ m high-resistive silicon, 300- μ m thickness quartz, and 300- μ m polycrystalline CVD diamond, to compare the electrical performance on each situation.

The principle of operation of the resistive switch is based on the application of a certain dc voltage between metal electrodes which allows to control the conduction state of the hBN layer. When a positive dc voltage is applied between metal electrodes, a conduction channel is created in the device allowing the current conduction, ON-state, also known as

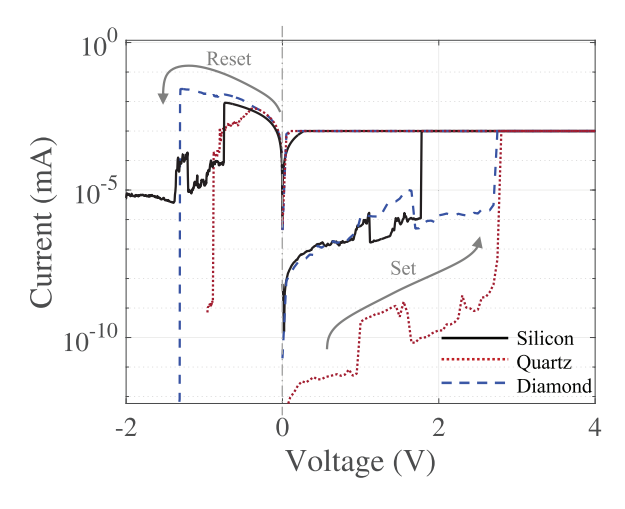


Fig. 3. Measured currents as a function of the applied voltage. Positive voltages are used to switch the device to the ON-state, while reversed polarity is used to turn the device to the OFF-state. The hysteresis cycle has been obtained for the switch on silicon (solid black), quartz (dotted red), and diamond (dashed blue) substrates.

SET state or low-resistivity state (LRS). In contrast, when a reversed polarity voltage is applied, the conduction channel is relived so the device is turn to the OFF-state in terms of conduction current, also known as RESET state or high-resistivity state (HRS). This is due to metal migration from the electrodes into the insulator in the form of conductive nanofilaments [18]. The full hysteresis cycle has been obtained for the three types of switch, applying a voltage sweep in the range from 0 to 4 V to set the device to the ON-state, and from 0 to -2 V (reversed polarity) to turn the device in the reset or OFF-state. Both the dc and RF signal fed the switch by means of a bias-tee allowing to obtain the S-parameters at any bias point condition. The switching time has also been measured with values <2.5 ns.

The measured currents are shown in Fig. 3. On one hand, it can be seen that the voltage to set the switch to the ON-state is below 1.8 V in case of using a silicon substrate, and a slightly higher, around 2.8 V in case of using quartz and diamond substrates. The maximum current has been limited to 1 μ A to prevent damage when the switch is set to the ON-state. On the other hand, the voltages to set the switch to the OFF-state are below -1.5 V in all the cases. In this case, since the channel is expected to be relieved, there is no need to limit the maximum current. As smaller is the measured current better the channel is relieved, and better isolation is expected to perform the switch. It has to be pointed that some variability in the floor current level has been observed by measuring one switch during several cycles.

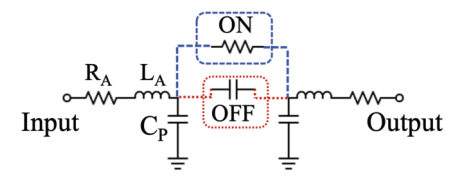


Fig. 4. Electric model for the ON/OFF-state of the resistive switch. R_A , L_A , and C_P correspond to the extrinsic part, modeling the coplanar access, while $R_{\rm ON}$ and $C_{\rm OFF}$ models the intrinsic part of the switch.

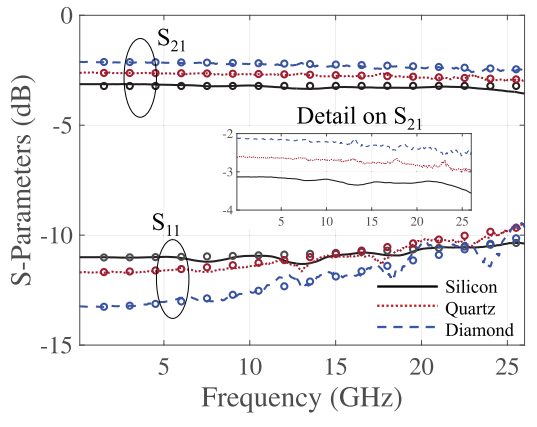


Fig. 5. Comparison between the electrical fit model (symbols) and the experimental measured data for insertion and return losses on different substrates (solid black) for the silicon, (red dotted) for the quartz, and (blue dashed) for diamond operating the switch in the ON-state.

The device has been electrically modeled considering RF coplanar access. The intrinsic part of the device can be characterized by means of a parallel $R_{\rm ON}$ – $C_{\rm OFF}$ tank in series configuration for the ON/OFF-state, respectively. The extrinsic part of the device can be modeled by means of a series resistance R_A , accounting for ohmic losses, a series inductance L_A for the small reactive behavior, and a shunt capacitance C_P which models parasitic couplings between ground and signal line in the coplanar structure as depicted in Fig. 4. The extracted elements for the switch on each substrate are equal since there the current leakage is minimum.

III. CHARACTERIZATION OF THE RESISTIVE SWITCHES AT HIGH FREQUENCIES

The different devices have been characterized in a frequency range from 10 MHz to 26.5 GHz. The input power level at RF frequencies has been set to -10 dBm to not interfere on the state of the switch, since high input power levels could switch the state of the memristor. The extrinsic parameters have been extracted by fitting the proposed electrical model to experimental measurements. All the substrates present a high resistivity, so ohmic losses due to metal electrodes are around 2.8 Ω in all the cases. The parasitic capacitance has been obtained around $C_P = 42$ fF, and the series inductance $L_A = 10$ pH. As depicted in Fig. 1, the signal line is tapered from 100 to 3 μ m of the active area which may lead to some mismatch losses.

Fig. 5 shows the characterization of the switch operating in the ON-state, thus allowing the signal to propagate between input and output ports. The measured ILs are below 2.5 dB

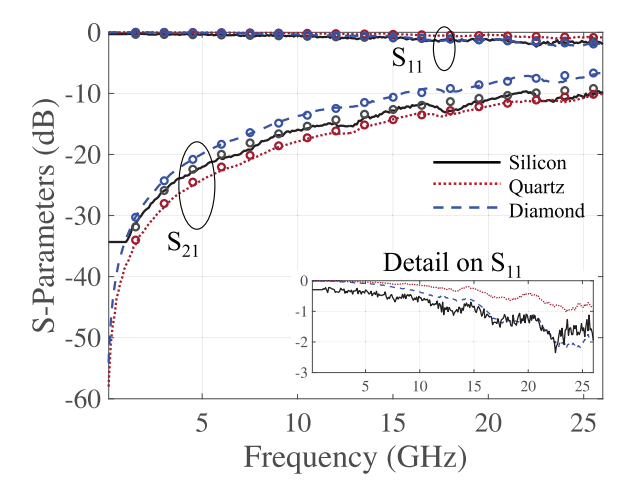


Fig. 6. Comparison between the electrical fit model (symbols) and the experimental measured data for insertion and return losses on different substrates (solid black) for the silicon, (red dotted) for the quartz, and (blue dashed) for diamond operating the switch in the OFF-state.

in case of diamond substrate (best case), and 3.5 dB for silicon (worst case) where part of them are due to impedance mismatch. The obtained channel resistance is $28~\Omega$ which is consistent with the results in [19], where a series resistance of approximately 1.4 Ω has been obtained by fitting the electrical model. It must be note that as previously commented, the structure in [19] is based on a single hBN layer, unlike the structure here containing 18 layers as depicted in Fig. 2. The associated channel resistance (and ILs) could be decreased by decreasing the number of layers of the hBN, and improving the manufacturing process.

The OFF/(reset) state has also been characterized in the entire RF frequency range as shown in Fig. 6. The obtained capacitance modeling the gap between contacts is approximately $C_{\rm OFF}=22$ fF. Isolation levels better than 10 dB are obtained for all the substrates, which may have some variability depending on how the channel is relived. Taking into account the characterization of the switch in the frequency domain for the ON- and OFF-states, it can be concluded that the device would have less impact in terms of ILs when used in a shunt configuration. With the measured parameters, the cutoff frequency of the devices is around 260 GHz, limited by $R_{\rm ON}$ and $C_{\rm OFF}$ values.

IV. CONCLUSION

In this article, the experimental characterization of resistive switches in a frequency range from 10 MHz to 26.5 GHz has been carried out. The switch, based on a multilayer hBN, has been fabricated on different substrates, high-resistivity silicon, quartz, and polycrystalline CVD diamond to compare the electrical performance. The dc hysteresis cycle for each device has been obtained showing activation voltages in the range of 1.8–2.8 V, and negative polarity around –1.5 V for the OFF-state. The devices have also been characterized at high frequencies. The series resistance in the ON-state has been obtained around 28 Ω . On the other hand, the capacitance in the OFF-state has been obtained to be 22 fF approximately which lead to a cutoff frequency of 260 GHz.

REFERENCES

- [1] G. M. Rebeiz and J. B. Muldavin, "RF MEMS switches and switch circuits," *IEEE Microw. Mag.*, vol. 2, no. 4, pp. 59–71, Dec. 2001.
- [2] N. Wainstein, G. Adam, E. Yalon, and S. Kvatinsky, "Radiofrequency switches based on emerging resistive memory Technologies—A survey," *Proc. IEEE*, vol. 109, no. 1, pp. 77–95, Jan. 2021.
- [3] J. Sobolewski and Y. Yashchyshyn, "State of the art sub-terahertz switching solutions," *IEEE Access*, vol. 10, pp. 12983–12999, 2022.
- [4] T. Singh, G. Hummel, M. Vaseem, and A. Shamim, "Recent advancements in reconfigurable mmWave devices based on phase-change and metal insulator transition materials," *IEEE J. Microw.*, vol. 3, no. 2, pp. 827–851, Apr. 2023.
- [5] J. Liu, N. Carels, and N. Peachey, "Characterization and analysis of RF switches in SOI technology for ESD protection," in *Proc. IEEE Int. Rel. Phys. Symp. (IRPS)*, Mar. 2022, pp. 1–5.
- [6] J.-P. Raskin, "Fully depleted SOI technology for millimeter-wave integrated circuits," *IEEE J. Electron Devices Soc.*, vol. 10, pp. 424–434, 2022
- [7] J. M. Carroll, "Using GaN FETs for high power RF switches," in *Proc. IEEE Compound Semiconductor Integr. Circuits Symp.*, Oct. 2008, pp. 1–4.
- [8] C. Florian, G. P. Gibiino, and A. Santarelli, "Characterization and modeling of RF GaN switches accounting for trap-induced degradation under operating regimes," *IEEE Trans. Microw. Theory Techn.*, vol. 66, no. 12, pp. 5491–5500, Dec. 2018.
- [9] J. Iannacci, M. Huhn, C. Tschoban, and H. Pötter, "RF-MEMS technology for 5G: Series and shunt attenuator modules demonstrated up to 110 GHz," *IEEE Electron Device Lett.*, vol. 37, no. 10, pp. 1336–1339, Oct. 2016.
- [10] L.-Y. Ma, N. Soin, M. H. M. Daut, and S. F. W. M. Hatta, "Comprehensive study on RF-MEMS switches used for 5G scenario," *IEEE Access*, vol. 7, pp. 107506–107522, 2019.
- [11] S. Pazos et al., "Memristive circuits based on multilayer hexagonal boron nitride for millimetre-wave radiofrequency applications," *Nature Electron.*, vol. 7, no. 7, pp. 557–566, Jul. 2024.
- [12] G. Slovin, N. El-Hinnawy, K. Moen, and D. Howard, "Phase-change material RF switches and monolithic integration in 180 nm RF-SOI CMOS processes," in *IEDM Tech. Dig.*, Dec. 2021, pp. 1–4.

- [13] T. Singh and R. R. Mansour, "Ultra-compact phase-change GeTe-based scalable mmWave latching crossbar switch matrices," *IEEE Trans. Microw. Theory Techn.*, vol. 70, no. 1, pp. 938–949, Jan. 2022.
- [14] N. El-Hinnawy et al., "A four-terminal, inline, chalcogenide phase-change RF switch using an independent resistive heater for thermal actuation," *IEEE Electron Device Lett.*, vol. 34, no. 10, pp. 1313–1315, Oct. 2013.
- [15] A. Léon et al., "RF power-handling performance for direct actuation of germanium telluride switches," *IEEE Trans. Microw. Theory Techn.*, vol. 68, no. 1, pp. 60–73, Jan. 2020.
- [16] T. Singh and R. R. Mansour, "Experimental investigation of performance, reliability, and cycle endurance of nonvolatile DC-67 GHz phase-change RF switches," *IEEE Trans. Microw. Theory Techn.*, vol. 69, no. 11, pp. 4697–4710, Nov. 2021.
- [17] I. Bettoumi, N. Le Gall, and P. Blondy, "Phase change material (PCM) RF switches with integrated decoupling bias circuit," *IEEE Microw. Wireless Compon. Lett.*, vol. 32, no. 1, pp. 52–55, Jan. 2022.
- [18] Z.-R. Xu, Y.-F. Ye, B. Xia, L.-S. Wu, J.-F. Mao, and Y.-Y. Jia, "Conductive bridging-based memristive RF switches on a silicon substrate," *IEEE Trans. Microw. Theory Techn.*, vol. 70, no. 1, pp. 24–34, Jan. 2022.
- [19] M. Kim et al., "Monolayer molybdenum disulfide switches for 6G communication systems," *Nature Electron.*, vol. 5, no. 6, pp. 367–373, May 2022.
- [20] M. Kim et al., "Analogue switches made from boron nitride monolayers for application in 5G and terahertz communication systems," *Nat. Electron.*, vol. 3, pp. 479–485, Aug. 2020.
- [21] S. J. Yang et al., "Reconfigurable low-voltage hexagonal boron nitride nonvolatile switches for millimeter-wave wireless communications," *Nano Lett.*, vol. 23, no. 4, pp. 1152–1158, Jan. 2023.
- [22] K. Zhu et al., "The development of integrated circuits based on twodimensional materials," *Nature Electron.*, vol. 4, no. 11, pp. 775–785, Nov. 2021.
- [23] J. B. Roldan et al., "Modeling the variability of Au/Ti/h-BN/Au memristive devices," *IEEE Trans. Electron Devices*, vol. 70, no. 4, pp. 1533–1539, Apr. 2023.
- [24] M. Kim et al., "Zero-static power radio-frequency switches based on MoS₂ atomristors," *Nature Commun.*, vol. 9, no. 1, p. 2524, Jun. 2018.